

Vesicles in a Poiseuille flow

Gerrit Danker¹, Petia M. Vlahovska², and Chaouqi Misbah¹

¹*Laboratoire de Spectrométrie Physique, UMR, 140 avenue de la physique, Université Joseph Fourier, and CNRS, 38402 Saint Martin d'Heres, France*

²*Thayer School of Engineering, Dartmouth College, 8000 Cummings Hall, Hanover NH 03755, USA**

(Dated: October 31, 2018)

Vesicle dynamics in unbounded Poiseuille flow is analyzed using a small-deformation theory. Our analytical results quantitatively describe vesicle migration and provide new physical insights. At low ratio between the inner and outer viscosity λ (i.e. in the tank-treading regime), the vesicle always migrates towards the flow centerline, unlike other soft particles such as drops. Above a critical λ , vesicle tumbles and cross-stream migration vanishes. A novel feature is predicted, namely the coexistence of two types of nonequilibrium configurations at the centreline, a bullet-like and a parachute-like shapes.

PACS numbers: 87.16.Dg 83.50.Ha 87.17.Jj f3.80.Lz 87.19.Tt

Keywords:

The motions of vesicles made of closed bilayer membranes in viscous flows have received increasing attention in recent years because of their relevance to understanding cell dynamics in the microcirculation. The unusual mechanical properties of the lipid bilayer membrane, such as fluidity, incompressibility and resistance to bending, give rise to a number of fascinating nonequilibrium features of vesicle micro-hydrodynamics. For example, in linear shear flow vesicles are predicted to exhibit different types of motion: (i) tank-treading (TT) (the fluid membrane rotates as a tank-tread, while the orientation angle of the vesicle remains fixed in time) [1, 2], (ii) tumbling (TB) [3, 4], (iii) vacillating-breathing (VB) (the long axis undergoes oscillation about the flow, while the shape shows breathing) [5]. Some of these behaviors have been confirmed experimentally [6, 7, 8]. Vesicle dynamics in linear flows is now fairly well understood [2, 5, 9, 10, 11, 12].

Quadratic flows such as the Poiseuille flow are quite common, especially in the blood circulatory system, yet the impact of flow curvature on vesicle dynamics is not well understood. Number of studies have focused on capillary flows, where the vesicle diameter is comparable to the channel size and lubrication effects control vesicle motion [13, 14], or vesicles near walls, where hydrodynamic interactions with the wall give rise to cross-stream migration (in a direction perpendicular to the flow) [15, 16]. Blood vessels such as arterioles, however, can be 10-50 times larger than the cell diameter. In this case, effects of flow curvature may become dominant. Vesicle dynamics in unbounded Poiseuille flow has been considered only to a limited extent, using two-dimensional numerical simulations [17]. Cross-stream migration has been observed, even in the absence of wall [17]. The physical mechanism behind this migration is related to the spatial variations

of shear rate that exists in quadratic flows: deformable particles tend to move towards regions with lower shear in order to minimize shape distortion [18]. Drops, for example, migrate towards or away the flow centerline depending on the viscosity ratio [18]. In the case of vesicles, however, details of the migration mechanism remain elusive and there are number of open questions: What is the role of flow curvature in cross-stream vesicle migration? Is there relation between the migration direction and the basic modes of vesicle dynamics (i.e. TT, VB and TB)? What physical parameters control vesicle migration? The development of a theory that can answer these questions represents a challenging task because not only the shape, but also the location of the vesicle is not known a priori, and it must be solved for in a consistent manner.

Problem formulation and solution: In a reference frame centered in the vesicle, a channel flow is written as

$$\mathbf{v}_0 = (-v_s - \dot{\gamma}y - \alpha y^2) \mathbf{e}_x, \quad (1)$$

where α is a measure of the curvature of the flow profile, $\dot{\gamma}$ is the local shear rate, which depends to the distance between the vesicle center and the flow axis, $\dot{\gamma} = 2y_0\alpha$, and v_s is the slip velocity (to be determined), which is the difference between the actual velocity of the vesicle center in the flow direction and the unperturbed flow.

At the length scales of the vesicle, water is effectively very viscous. Hence, the total flow field $\mathbf{v} = \mathbf{v}_0 + \mathbf{u}$ (imposed flow \mathbf{v}_0 plus perturbation \mathbf{u} due to the presence of the vesicle) obeys the Stokes equations inside and outside the vesicle

$$\nabla p = \eta_i \nabla^2 \mathbf{v}, \quad \nabla \cdot \mathbf{v} = 0, \quad (2)$$

where η_i ($i = 1, 2$) is the fluid viscosity; η_1, η_2 are the internal and external viscosities, and $\lambda \equiv \eta_1/\eta_2$ is a measure of the viscosity contrast.

Assuming a nearly spherical shape, the solution to the creeping-flow equations is obtained as a regular perturbation expansion in the excess area, which is the

*chaouqi.misbah@ujf-grenoble.fr

difference in the areas of the vesicle and an equivalent sphere (with radius r_0) with the same volume, i.e., $\Delta = A/r_0^2 - 4\pi$. From the definition of the area it is evident that Δ is a quadratic function of the shape deviation from sphere. Thus it is convenient to set $\epsilon = \Delta^{1/2}$ as a formal expansion parameter. A time-dependent vesicle configuration is described by

$$\mathbf{R} = \mathbf{R}_0 + r_0[1 + \epsilon f(t, \theta, \phi)] \mathbf{e}_r, \quad (3)$$

where $\mathbf{R}_0 = (x_0, y_0, z_0)$ is the time-dependent position of the centroid of the vesicle and f describes shape deviation from the spherical shape. θ and ϕ are spherical coordinates. The vesicle shape $f(\theta, \phi)$ can be decomposed in an infinite series of spherical harmonics $Y_{lm}(\theta, \phi)$ excluding the $l = 1$ mode (which describes the translation $\dot{\mathbf{R}}_0$):

$$f = \sum_{l \neq 1} f_l = \sum_{l \neq 1} \sum_{m=-l}^l F_{lm}(t) Y_{lm}(\theta, \phi). \quad (4)$$

The amplitudes $F_{lm}(t)$ describe the shape evolution. For the present study (leading order analysis) it is sufficient to include the $l = 0$ mode, which ensures volume conservation, and the $l = 2, 3$ modes, which are excited by the imposed Poiseuille flow.

The velocity field is given by the classical Lamb solution [19]. This solution contains integration factors which are determined from the boundary conditions. These are: (i) Continuity of the fluid velocity across the membrane (valid if impermeability is assumed). (ii) Continuity of the stress across the membrane: the jump of fluid stress across the membrane is balanced by the membrane force. The latter consists of a normal force due to resistance to bending, and a tangential (fictitious) force, which originates from a Lagrange multiplier enforcing local membrane incompressibility. (iii) Local membrane incompressibility, which restricts the surface velocity field to be solenoidal. We have solved the full hydrodynamic problem in the same spirit as in the calculation for the linear shear flow. Details can be found in [12]; here we focus solely on the results and discuss the physical implications.

It should be noted that in certain cases, e.g., drops, the migration velocity can be obtained using a simplified approach based on the Lorentz reciprocal theorem [20]. However, this approach is inapplicable to vesicles because of the tangential membrane force.

Results and Discussion: The time evolution of the shape function ($\partial_t f$) together with the motion of the vesicle center with respect to the flow ($\dot{\mathbf{R}}_0$) are computed from the kinematic condition, which requires that the membrane moves with the fluid velocity. We find for the evolution of the $l = 2, 3$ (which are the only excited modes at leading order) the following equations:

$$\epsilon \mathcal{D}_t F_{2m} = -\frac{24(\sigma_0 + 6\kappa)}{23\lambda + 32} F_{2m} + \frac{i\alpha y_0}{23\lambda + 32} N_{2m}, \quad (5)$$

$$\epsilon \mathcal{D}_t F_{3m} = -\frac{120(\sigma_0 + 12\kappa)}{76\lambda + 85} F_{3m} + \frac{\alpha r_0}{76\lambda + 85} N_{3m} \quad (6)$$

with $\mathcal{D}_t = \partial_t + im\alpha y_0$, and $N_{20} = N_{2,\pm 1} = 0$, $N_{2,\pm 2} = \pm 8\sqrt{30\pi}$, $N_{30} = N_{3,\pm 2} = 0$, $N_{3,\pm 1} = \mp 5\sqrt{21\pi}/3$, $N_{3,\pm 3} = \mp 5\sqrt{35\pi}$. κ is the membrane bending rigidity rescaled by r_0^3/η . The evolution equations (5, 6) contain the tension-like quantity σ_0 , which is the homogeneous part of the Lagrange multiplier [2, 12]. Its value is computed from the condition that the shape deformation complies with the available excess area. σ_0 is easily determined from the above equations, and the expression relating excess area and the shape modes F_{lm} , as explained in [12].

Knowledge of the shape evolution allows us to compute the lateral (cross-stream) migration along the y -direction

$$\begin{aligned} v_m = & \frac{i}{4} \sqrt{\frac{30}{\pi}} \alpha \epsilon r_0^2 \frac{36\lambda + 71}{(\lambda + 4)(76\lambda + 85)} (F_{22} - F_{2,-2}) \\ & + \frac{16}{7} \sqrt{\frac{21}{\pi}} \frac{\alpha \epsilon r_0 y_0}{23\lambda + 32} (F_{31} - F_{3,-1}) \\ & + \frac{48}{7} \sqrt{\frac{35}{\pi}} \frac{\alpha \epsilon r_0 y_0}{23\lambda + 32} (F_{33} - F_{3,-3}). \end{aligned} \quad (7)$$

This equation is coupled back to the shape, leading to some interesting dynamics. First, in contrast to drops, a vesicle always migrates towards the centerline. Second, the migration velocity depends in a non-trivial way on the viscosity ratio and excess area.

For $\lambda < \lambda_c$, a numerical solution of the coupled equations for the shape (5, 6) and the migration (7) yields the usual tank-treading ellipsoid as long as the vesicle is far from the centerline, because the linear shear dominates over the quadratic component of the flow. The latter, however, induces migration towards the center of the flow. As the vesicle moves its shape deforms more and more until it becomes a parachute (or assumes another shape, namely bullet-like, as discussed below) when the centerline is reached (Fig. 1). The migration velocity far

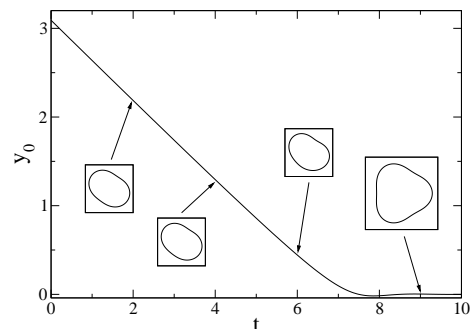


FIG. 1: Evolution of the vertical position of the vesicle as a function of time. Some snapshots of the vesicle shape along the trajectory are shown as insets. Parameters: $\alpha = 6, \kappa = 1, \Delta = 0.25$.

from the centerline is well approximated by plugging the solution for the tank-treading ellipsoidal shape, $R = \epsilon/2$, $\cos 2\psi = \epsilon/2h$ with R and ψ defined by $\epsilon F_{22} = R e^{-i2\psi}$

into Eq. (7) [5].

$$v_m = -\frac{17284\lambda^2 + 66671\lambda + 55840}{60(\lambda + 4)(23\lambda + 32)(76\lambda + 85)}\sqrt{\frac{30}{\pi}}\alpha\Delta^{1/2}r_0^2. \quad (8)$$

For $\lambda \sim 1$ the migration velocity is approximately $v_y = -0.16\alpha\Delta^{1/2}r_0^2$. In a typical experiment in a rectangular microchannel we have $\alpha \sim 0.3(\mu\text{m}\cdot\text{s})^{-1}$, $\Delta = 0.25$, $r_0 = 20\mu\text{m}$, and a migration velocity of $0.75\mu\text{m/s}$ [21]. Using Eq. (8), we find an expected migration velocity of about $1\mu\text{m/s}$. Note also that (8) is independent of the membrane bending rigidity. This is understood as follows. The local shear rate is proportional to the distance from the centerline: $\dot{\gamma} \sim y_0$. The elongational component of the flow (which increases like the shear rate) must be compensated by the membrane tension in order to fulfil local membrane incompressibility. It follows that the tension σ_0 must also scale like y_0 . Then, for large y_0 , the terms 6κ and 12κ in Eqs. (5, 6) become negligible and the membrane dynamics becomes independent of κ .

The direction of the lateral migration of the vesicle in Poiseuille flow can intuitively be understood from the following argument. Assume that we have solved the problem for the pure shear flow, $\dot{\gamma}(y_0)y$. The solution is the tank-treading vesicle shown in Fig. (2). Next, we add the

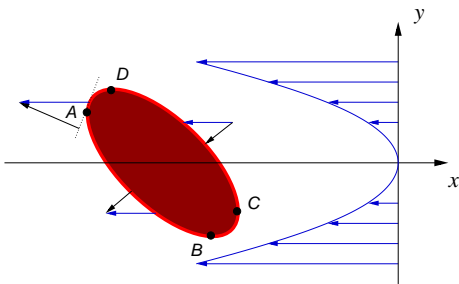


FIG. 2: (Color online) A vesicle in Poiseuille flow far from the centerline. The local velocity field can be decomposed into a local shear $\dot{\gamma}(y_0)$ (responsible for the tank-treading vesicle at the shown orientation) and a (small) quadratic correction (blue arrows). Due to the inclination of the vesicle long axis with respect to the quadratic flow field, there is a net force acting on the vesicle membrane in the negative y direction.

quadratic correction $-\alpha y^2$ as a perturbation. The additional flow, acting on the membrane of the vesicle, can be decomposed into two components: one tangential to the membrane, which locally modifies the tank-treading velocity, and one normal to the membrane, which modifies the vesicle shape and possibly cause migration. In the segments AB and CD the perpendicular component tends to push the vesicle into the negative y direction, whereas in the smaller segments DA and BC , the perpendicular component pushes the vesicle in the positive y direction. As the segments AB and CD account for most of the vesicle's surface, the net force has a component in the negative y direction (towards the flow centerline).

Let us turn now to the problem of migration in the tumbling regime. From the analytical results discussed

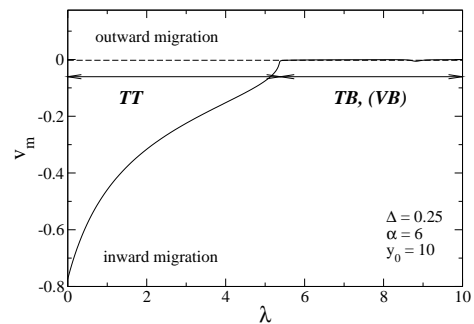


FIG. 3: Migration velocity as a function of the viscosity contrast λ for the various regimes: tank-treading (TT), tumbling (TB), and vacillating-breathing (VR)

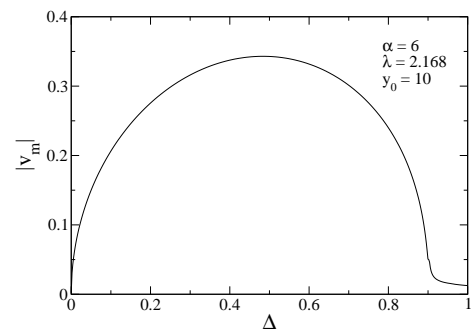


FIG. 4: Migration velocity as a function of the excess area far from the centerline. Parameters are chosen such that the tank-treading regime stops at $\Delta = 0.9$.

above for the tank-treading regime, one finds that the migration velocity close to the tumbling regime (which occurs at $\lambda = \lambda_c$ [5]) behaves as $\sqrt{\lambda - \lambda_c}$, and thus it vanishes exactly at the threshold. This analysis is valid on the tank-treading side. For $\lambda > \lambda_c$, the vesicle tumbles, and in this case we have integrated numerically the set of equations (5,6,7). The migration (averaged over time) is again always towards the flow centerline but the magnitude of the migration velocity is very close to zero (of the order of $10^{-2}r_0$ per tumbling cycle). The results are shown on Fig.3. For large viscosity ratios, $\lambda \gg 1$, the migration velocity must go to zero, since the vesicle behaves as a rigid sphere. The kinematic reversibility of the Stokes equations precludes a lateral migration in this case. This feature is also evident from the expression for the migration velocity (7). Indeed, the F'_{ij} s are finite due to the constraint of fixed excess area, but the prefactors $O(\lambda^{-1})$. Thus, when $\lambda \rightarrow \infty$, $v_m \rightarrow 0$.

An interesting feature is the non-monotonic dependence of the migration velocity on the excess area Δ , see Fig. 4. For a spherical object (i.e., $\Delta = 0$) one has no migration, $v_m = 0$, due to the up-down symmetry. If viscosity is large enough so that tumbling becomes possible for a sufficiently deflated vesicle, then we similarly expect $v_m \sim 0$, for high enough Δ . Hence,

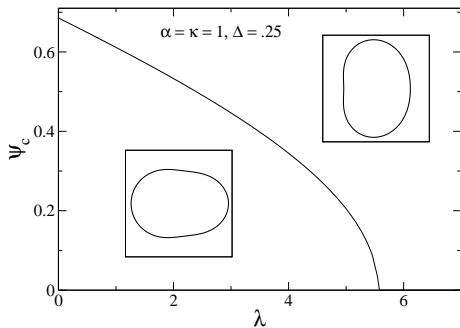


FIG. 5: Critical angle ψ_c separating the basins of attraction for two coexisting solutions at the centerline.

it follows that the absolute value of the migration velocity attains a maximum for a certain value of Δ as illustrated in Fig. 4. This results also agrees with the argument given on the lift force under a linear shear flow[15]. Vesicle approach to the flow centerline also can proceed in a non-monotonous manner. the ratio $\eta_0 R_0^4 \alpha / \kappa$ (this is a measure of the relative strength of hydrodynamic and bending stresses) is sufficiently large (typically above 10), the vesicle approaches the centerline monotonously. However, for smaller curvature of the flow field (or higher membrane rigidity) the vesicle trajectory exhibits damped oscillations about the centerline. For typical values $\alpha \sim 0.1(\mu\text{ms})^{-1}$, $R_0 \sim 10\mu\text{m}$, and by using the viscosity of water and $\kappa \sim 40k_B T$, one finds that $\eta_0 R_0^4 \alpha / \kappa \sim 0.1$. This means these damped oscillations should be easily observed experimentally.

A new surprising feature we have discovered is the coexistence of shape solutions at the centerline for small

enough curvature of the flow field (see Fig. 5). More precisely, this occurs if $\eta_0 R_0^4 \alpha / \kappa$ is lower than about 4 – 5. For one solution the longest axis of the vesicle is oriented in the flow direction (bullet-like shape), and for the other one it is perpendicular to it (parachute-like shape). Each of these solutions has its own basin of attraction, i.e., if the initial angle at the centerline is smaller than ψ_c , the bullet-like shape is attained, and otherwise the parachute-like shape. If, however, the curvature of the flow is strong enough, the vesicle will assume a pronounced parachute-like shape, and the two solutions will be indistinguishable. We hope to report further on this matter in a future work. The experimental range that is relatively easily accessible is about[21] $10^{-1} < \eta_0 R_0^4 \alpha / \kappa < 10$. This means that in principle this prediction is not devoid of experimental testability. The challenge is to orient the vesicle in the appropriate basin of attraction. Optical tweezers constitute a possible tool for this task. The slip velocity for the parachute-like shape is higher, while for a bullet-like vesicle is lower than that of a rigid sphere, $v_s = -1/3 \alpha r_0^2$ (as deduced from Faxen's law [22]). Since the slip velocity for the bullet-shape is smaller than that of the parachute the dissipation implied by this morphology should be lower.

In summary, the dynamical behavior of a vesicle in unbounded quadratic flow has revealed number of novel features that stem from the subtle interplay between membrane mechanics and shear gradients due to flow curvature. The analysis has been also performed for an axisymmetric Poiseuille flow and yields the same qualitative results.

C.M. Acknowledges financial support from CNES (Centre National d'Etudes Spatiales) and ANR (MOSICOB project).

-
- [1] M. Kraus, W. Wintz, U. Seifert, and R. Lipowsky, Phys. Rev. Lett. **77**, 3685 (1996).
 - [2] U. Seifert, Eur. Phys. J. B. **8**, 405 (1999).
 - [3] S. R. Keller and R. Skallak, J. Fluid Mech. **120**, 27 (1982).
 - [4] T. Biben, C. Misbah, Phys. Rev. E **67**, 031908 (2003).
 - [5] C. Misbah, Phys. Rev. Lett. **96**, 028104 (2006).
 - [6] K. de Haas, C. Bloom, D. van den Ende, M. Duits, J. Mellema, Phys. Rev. E **56**, 7132 (1997).
 - [7] V. Kantsler and V. Steinberg, Phys. Rev. Lett. **95**, 258101 (2005), **96**, 036001 (2006). (2006).
 - [8] M. Mader, V. Vitkova, M. Abkarian, A. Viallat, and T. Podgorski, Eur. Phys. J. E. **19**, 389 (2006).
 - [9] P. M. Vlahovska and R. S. Gracia, Phys. Rev. E **75**, 016313 (2007).
 - [10] H. Noguchi and G. Gompper, Phys. Rev. Lett. **98**, 128103 (2007).
 - [11] V. V. Lebedev, K. S. Turitsyn, and S. S. Vergeles, Phys. Rev. Lett. **99**, 218101 (2007).
 - [12] G. Danker, T. Biben, T. Podgorski, C. Verdier, and C. Misbah, Phys. Rev. E (2007).
 - [13] V. Vitkova, and M. Mader, and T.M. Podgorski, Europhys. Lett. **68**, 398 (2004).
 - [14] H. Noguchi and G. Gompper. PNAS **102**, 14159 (2005).
 - [15] P. Olla J. Phys. II (France) **7**, 1533 (1997); Physica A **278**, 87 (2000).
 - [16] M. Abkarian and A. Viallat. Biophys. J. **89**, 1055 (2005).
 - [17] B. Kaoui, G. H. Ristow, I. Cantat, C. Misbah, and W. Zimmermann, Phys. Rev. E **77**, 021903 (2008).
 - [18] L. G. Leal, Annu. Rev. Fluid Mech. **12**, 435 (1980).
 - [19] H. Lamb, Hydrodynamics, 6th edition, Cambridge Univ. Press, 1932.
 - [20] P.C-H. Chan, and L.G. Leal, J. Fluid Mech. **92**, 131 (1979).
 - [21] G. Coupier. Private communication.
 - [22] L. G. Leal, *Advanced Transport Phenomena*, Cambridge University Press (2007)